Title
Kif2a Scales Meiotic Spindle Size in Hymenochirus boettgeri.

Journal
Current Biology, 29(21)

Authors
Miller, Kelly
Session, Adam
Heald, Rebecca

Publication Date
2019-11-04

DOI
10.1016/j.cub.2019.08.073

Peer reviewed

Published in final edited form as:

Curr Biol. 2019 November 04; 29(21): 3720–3727.e5. doi:10.1016/j.cub.2019.08.073.

Kif2a scales meiotic spindle size in *Hymenochirus boettgeri*

Kelly E. Miller[1], **Adam Session**[1], **Rebecca Heald**[1,*]

[1]Department of Molecular and Cell Biology, University of California, CA 94720, Berkeley, USA

Summary

Size is a fundamental feature of biological systems that affects physiology at all levels. For example, the dynamic, microtubule-based spindle that mediates chromosome segregation scales to a wide range of cell sizes across different organisms and cell types. *Xenopus* frog species possess a variety of egg and meiotic spindle sizes, and differences in activities or levels of microtubule-associated proteins in the egg cytoplasm between *Xenopus laevis* and *Xenopus tropicalis* have been shown to account for spindle scaling [1]. Increased activity of the microtubule severing protein katanin scales the *X. tropicalis* spindle smaller compared to *X. laevis* [2], as do elevated levels of TPX2, a protein that enriches the cross-linking kinesin-5 motor Eg5 at spindle poles [3]. To examine the conservation of spindle scaling mechanisms more broadly across frog species, we have utilized the tiny, distantly related Pipid frog *Hymenochirus boettgeri*. We find that egg extracts from *H. boettgeri* form meiotic spindles similar in size to *X. tropicalis*, but that TPX2 and katanin-mediated scaling is not conserved. Instead, the microtubule depolymerizing motor protein kif2a functions to modulate spindle size. *H. boettgeri* kif2a possesses an activating phosphorylation site that is absent from *X. laevis*. Comparison of katanin and kif2a phosphorylation sites across a variety of species revealed strong evolutionary conservation, with *X. laevis* and *X. tropicalis* possessing distinct and unique alterations. Our study highlights the diversity and complexity of spindle assembly and scaling mechanisms, indicating that there is more than one way to assemble a spindle of a particular size.

eTOC blurb

Miller *et al*. use an egg extract system from the tiny frog *Hymenochirus boettgeri* to show that mechanisms that mediate meiotic spindle size differences in Pipid frogs are not conserved at the level of the genus. Instead, a novel mechanism is proposed involving differential phosphorylation of the microtubule depolymerizing kinesin kif2a.

Graphical Abstract

*Corresponding author: bheald@berkeley.edu.

Author contributions

R.H and K.M. designed the project. K.M. performed all experiments and analyzed the data. A.S. assembled the *H. boettgeri* transcriptome, and performed searches and amino acid alignments of katanin and kif2a in multiple species. K.M. prepared the figures, and R.H. and K.M. wrote the manuscript, with input from A.S.

Declaration of Interests

The authors declare no competing interests.

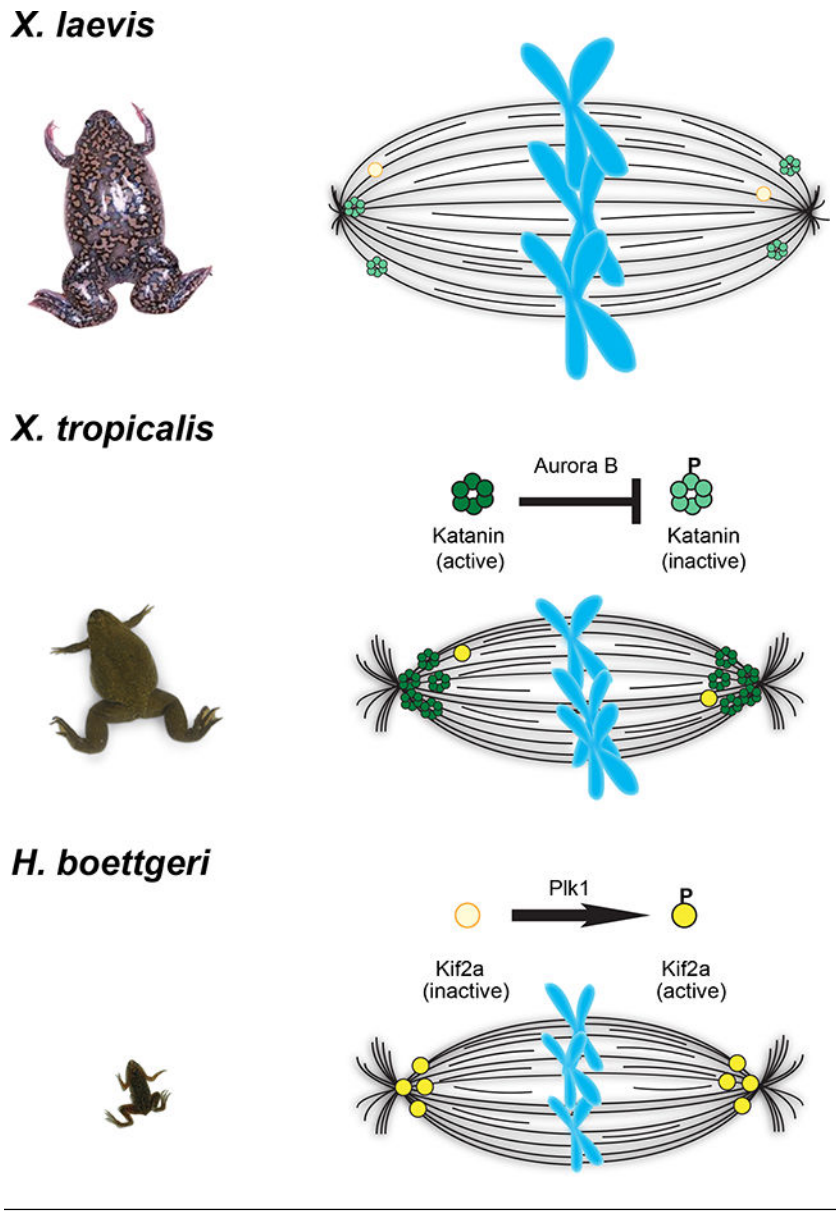

Results

H. boettgeri egg extracts recapitulate spindle assembly in vitro

To investigate whether the scaling mechanisms previously identified between *X. laevis* and *X. tropicalis* are conserved at the level of the genus, we developed an egg extract system from the African Dwarf frog *Hymenochirus boettgeri*, which to date has been poorly studied relative to its *Xenopus* counterparts and is best known in the pet trade. The *Hymenochirus* and *Xenopus* genera diverged over 110 MYA [4,5]. The body weight of *H. boettgeri* averages only 2 grams- about 1/15th the average weight of *X. tropicalis*, and 1/45th that of the larger *X. laevis* (Figure S1A). *H. boettgeri* eggs average ~684 μm in diameter, compared to *X. tropicalis* at 800 μm, and *X. laevis* at 1189 μm, corresponding to an overall ~5-fold difference in volume (Figure 1A). Interestingly, although *H. boettgeri* eggs are significantly

smaller than those of *X. tropicalis*, spindle lengths are similar in both species, with averages of 23 and 24 μm, respectively (Figure 1B).

In order to identify factors involved in spindle size control in *H. boettgeri*, we developed an egg extract system similar to that of *Xenopus* that is subject to cell cycle control and amenable to biochemical manipulation. Although extract preparation was challenging due to the small size of the eggs and required the ovulation of at least 8–12 frogs per extract, the system robustly recapitulated events of the cell cycle such as meiotic spindle assembly (Figure 1C) and formation of interphase nuclei (unpublished data). The architecture of spindle microtubules in *H. boettgeri* eggs and extracts appeared slightly different from that of the *Xenopus* species, with increased microtubule density at the poles relative to the central spindle (Figure 1B, 1C). Spindles formed in *H. boettgeri* extracts were statistically similar in length to meiotic spindles in the egg, indicating that extract conditions faithfully reproduced in vivo spindle size (Figure 1D).

Spindle size scaling in *H. boettgeri* egg extracts

Addition of *H. boettgeri* egg extracts to *X. laevis* egg extracts reduced spindle length in a dose-dependent manner (Figure 2A), suggesting that not only are egg extracts from two entirely different frog genera compatible enough to assemble spindles, but also that cytoplasmic factors are responsible for controlling spindle size.

To determine whether mechanisms of spindle size control previously identified in *Xenopus* are conserved in *H. boettgeri*, we examined TPX2 and katanin as candidate spindle scaling factors. In *X. tropicalis* egg extracts, TPX2 is present at 2–3-fold higher levels than in *X. laevis* egg extracts and is highly enriched on spindle microtubules. Increased TPX2-mediated recruitment of Eg5 is thought to increase parallel microtubule cross-linking at spindle poles, thereby decreasing spindle length [3]. In comparison, TPX2 did not localize as intensely to spindle microtubules in *X. laevis* and *H. boettgeri* egg extracts (Figure 2B). By immunoblot TPX2 levels in *H. boettgeri* egg extracts were similar to those in *X. laevis* (Figure 2C) and Eg5 was not enriched at spindle poles as observed in *X. tropicalis* egg extracts ([3], unpublished data), indicating that TPX2 does not function to reduce meiotic spindle size in *H. boettgeri*.

A second spindle scaling mechanism operating in *Xenopus* is altered microtubule depolymerization rates, which were shown to be higher in *X. tropicalis* egg extracts due to differential regulation of the microtubule severing enzyme katanin. Katanin concentrates at spindle poles in *X. tropicalis* where it is thought to promote depolymerization by severing microtubules along their length, as well as by promoting kinesin-13 driven depolymerization of newly exposed microtubule ends [6,7]. The *X. laevis* homolog of katanin contains a serine reside at amino acid 131 of its catalytic p60 subunit, which is phosphorylated and inhibited by Aurora B kinase. In contrast, the *X. tropicalis* homolog of p60 katanin possesses a glycine residue at this position, thereby blocking phosphorylation and increasing microtubule severing rates [2]. Interestingly, although the *H. boettgeri* homolog of p60 katanin is 88% identical to that of *X. tropicalis* and 89% identical to *X. laevis*, (Figure S1B), it possesses the predicted Aurora B phosphorylation site at serine 131 (Figure 2D), and microtubule severing rates in *H. boettgeri* egg extracts were qualitatively similar to those in

X. laevis (Figure 2E). Therefore, it is unlikely that katanin is responsible for the reduced spindle size in *H. boettgeri* egg extracts.

Serine 252 of kif2a modulates spindle size in *H. boettgeri*

Kif2a, a microtubule depolymerizing motor protein of the kinesin 13 family, was previously identified as a spindle scaling factor that operates during early *X. laevis* development, when rapid cell cleavages give rise to smaller and smaller cells [8]. We therefore investigated a potential role for kif2a in spindle size scaling in *H. boettgeri*. Kif2a antibodies stained *H. boettgeri* spindles more intensely compared to *X. laevis* and *X. tropicalis* (Figure 3A), although levels of kif2a were similar in egg extracts of all three species (Figure 3B). Whereas inhibition of kif2a in *X. laevis* eggs and early embryos was not observed to affect spindle length ([8] and unpublished data), addition of an inhibitory anti-kif2a antibody to *H. boettgeri* egg extracts caused an increase in spindle size as well as spindle microtubule density (Figure 3C). These observations indicated a role for kif2a as a scaling factor in an interspecies rather than a developmental context.

To determine whether the *H. boettgeri* homolog of kif2a contributed to spindle length scaling, we added purified recombinant kif2a proteins (Figure S2A) to *X. laevis* egg extracts. Whereas addition of *H. boettgeri* kif2a decreased spindle length by ~25%, addition of an equal amount of *X. laevis* kif2a had a much lesser effect (Figure 4A). The kif2a protein is comprised of a conserved central catalytic domain flanked by N and C terminal regions that mediate dimerization and subcellular targeting [9,10]. Sequence alignment of the *H. boettgeri* and *X. laevis* kif2a homologs revealed 93.6% identity (Figure S2B). To test whether minor sequence variations contributed directly to differences in microtubule depolymerization by the kif2a homologs, we compared activity of the recombinant proteins in a microtubule pelleting assay (Figure 4B). *H. boettgeri* and *X. laevis* kif2a possessed very similar activities in shifting tubulin subunits to the supernatant, implicating a post-translational modification in their differential activity regulating spindle length.

Close inspection of kif2a sequences revealed a potential regulatory site at serine 252 within the catalytic domain of *H. boettgeri* kif2a. In human cells this residue was previously implicated as a site phosphorylated by Polo-like-kinase 1 (Plk1), a kinase shown to activate the microtubule depolymerizing activity of kif2a [11]. However, the *X. laevis* kif2a homolog contains an isoleucine residue at position 252 (I252), which cannot be phosphorylated (Figure 4C). Addition of a mutant version of the *X. laevis* kif2a containing a serine residue at this site (Kif2a I252S) to *X. laevis* egg extracts caused a dramatic reduction in spindle length, similar to that observed when an equal concentration of recombinant wild type *H. boettgeri* kif2a was added. A similar effect was observed when a phosphomimetic mutant version of the *X. laevis* kif2a containing a glutamic acid residue at this site (Kif2a I252E) was added to extracts (Figure S3A). Interestingly, this mutant did not show increased intensity at spindle poles compared to wild type *X. laevis* kif2a, indicating that increased kif2a activity rather than concentration leads to the reduction in spindle length (Figure S3B). Conversely, addition of *H. boettgeri* kif2a in which the serine was substituted with an isoleucine at position 252 (Kif2a S252I) reduced spindle length to a lesser degree, which was similar to the activity of wild type *X. laevis* kif2a (Figure 4D). These results identify

kif2a phosphorylation and activation as the likely mechanism scaling spindles smaller in *H. boettgeri* compared to *X. laevis*. Interestingly, the phosphomimetic version of kif2a did not possess greater microtubule depolymerizing activity towards pure microtubules than the wild-type version, suggesting that phosphorylation of serine 252 on its own is not sufficient to activate kif2a (unpublished data). Future experiments will address whether other modifications or interacting factors act to modulate kif2a activity in vivo.

Conserved constellations of spindle scaling factors operate across species

Taken together, our results suggest that mechanisms of interspecies spindle scaling identified in *Xenopus* are not conserved at the level of the genus in the more distantly related frog *Hymenochirus boettgeri*. However, commonalities exist among spindle scaling mechanisms across frog species that involve microtubule destabilizing factors and their regulation by mitotic kinases. To examine the evolutionary conservation of spindle scaling activities by microtubule depolymerizing factors, we compared the regulatory phosphorylation sites of kif2a and katanin across a variety of species (Figure S4). Interestingly, all species examined except for *X. laevis* contained the activating serine at residue 252 of kif2a, suggesting that reduced activity of kif2a is unique to *X. laevis*. Moreover, only *X. tropicalis* katanin possessed the inhibitory serine at position 131. These observations suggest that spindle size control mechanisms are overall evolutionary conserved, but that some species are “outliers” that possess distinct mechanisms setting meiotic spindle length.

Discussion

Our study reveals that distinct mechanisms operate across frog species to set meiotic spindle length. Whereas high levels of TPX2 and the absence of an inhibitory phosphorylation site on katanin scales the *X. tropicalis* spindle smaller than that of *X. laevis*, an activating phosphorylation site on *H. boettgeri* kif2a appears to be crucial for setting meiotic spindle size in this tiny species.

Thus, to date, three meiotic spindle scaling factors including TPX2, katanin, and kif2a have been identified. Previous computational simulations evaluating the microtubule dynamic parameters that set meiotic spindle length indicated that the activity of depolymerizers such as kif2a or microtubule severing enzymes such as katanin could operate primarily at microtubule minus ends, which are enriched at spindle poles [12]. Although our study implicates kif2a phosphorylation in regulating its activity, differences in localization may also play a role. In addition to modulating spindle length, variation among spindle factors and their regulators likely contributes to differences in spindle architecture across species [13].

Interestingly, with respect to phosphoregulatory sites on katanin and kif2a, there is not a clear correlation between their presence or absence and spindle size. For example, *Xenopus borealis*, which is similar to *X. laevis* in terms of genome and egg size, forms meiotic spindles of similar length to *X. laevis*, yet possesses both the inhibitory phosphorylation site of *X. laevis* katanin and the activating phosphorylation site found in *X. tropicalis* and *H. boettgeri* kif2a (Figure S4, [13]). This suggests that other factors or regulatory mechanisms operate, which could differentially set the activity of mitotic kinases Aurora B and Polo, or

affect the small GTPase Ran, which functions through importins to regulate a number of spindle assembly factors. Observed differences in meiotic spindle morphology and microtubule distribution along the length of the spindle of multiple frog species, as well as sensitivity to Ran disruption, highlight many possible variations in spindle architecture and assembly mechanisms. Furthermore, other factors such as the microtubule polymerase XMAP215 and microtubule cross-linking motors have also been shown to regulate spindle length [14],[15]. Future studies will shed light on how the collective activities and regulation of a suite of factors can generate spindles with distinct architectures and sizes.

An important open question is the importance of spindle size for chromosome segregation. Experiments decreasing mitotic spindle length through manipulation of kif2a in *X. laevis* embryos caused defects in metaphase spindle alignment, but spindle orientation defects were corrected in anaphase and cleavage divisions were not disrupted [8], suggesting that astral microtubule growth rather than metaphase spindle length plays a crucial role. Of note, while *X. laevis, X. tropicalis*, and *H. boettgeri* scale in size at the level of the organism, egg, and genome, the *H. boettgeri* meiotic spindle size is very similar to that of *X. tropicalis*. Furthermore, a comparison of meiotic spindle morphometrics across many species did not reveal a strong correlation between egg size and spindle length, which possesses a narrow range compared to mitotic spindle size [16]. One possibility is that there is a lower limit to meiotic spindle size in amphibian eggs, and has this been reached in frogs as small as *X. tropicalis* and *H. boettgeri*. Manipulation of meiotic spindle size in vivo will be required to address this question.

Why have rare variations in spindle scaling factor sequences evolved in *X. laevis* katanin and *X. tropicalis* kif2a? Did these changes provide a fitness advantage, or did other changes compensate for them? It is interesting that the *X. borealis* kif2a sequence resembles that of the ancestral, *X. tropicalis*-like species prior to polyploidization, while the sequence in *X. laevis*, which is much more closely related to *X. borealis*, has diverged. Yet uncharacterized changes in spindle size control mechanisms in *X. borealis* may accommodate the increase in genome size in this species. Surveying sequence and expression levels of spindle size control factors over a diverse range of amphibian species promises to reveal whether additional mechanisms have evolved together with changes in ploidy to mediate spindle scaling.

In conclusion, in vitro frog egg extract systems provide a system to explore spindle assembly mechanisms as well as evolutionary forces and constraints that affect size scaling.

STAR Methods

Lead Contact and Materials Availability

Further information and requests for resources and reagents should be directed to and will be fulfilled by the Lead Contact, Rebecca Heald (bheald@berkeley.edu). In general, plasmid constructs and antibodies are available for sharing.

Experimental model and subject details

All frogs were used and maintained in accordance with standards established by the Animal Care and Use Committee (ACUC) at the University of California, Berkeley. Mature *X. laevis*

and *X. tropicalis* frogs were obtained from NASCO (Fort Atkinson, WI). Mature *H. boettgeri* frogs were obtained from Albany Aquarium (Albany, CA). *Xenopus* frogs were housed in a recirculating tank system with regularly monitored temperature and water quality (pH, conductivity, and nitrate/nitrite levels). *Xenopus laevis* were housed at a temperature of 20–23 °C, and *Xenopus tropicalis* housed at 23–26 °C. *H. boettgeri were* housed in a static tank system at 23–25 °C with regular water changes and regularly monitored water quality as for the *Xenopus*. All animals were fed Nasco frog brittle.

Whole mount immunofluorescence of *X. laevis, X. tropicalis*, and *H. boettgeri* eggs

Dejellied eggs were fixed for one hour using MAD fixative (2 parts methanol [Thermo Fisher Scientific], 2 parts acetone [ThermoFisher Scientific], 1 part DMSO [Sigma]). After fixation, eggs were dehydrated in methanol and stored at −20°C. Eggs were then processed as previously described [17] with modifications. Following gradual rehydration in 0.5X SSC (1X SSC: 150 mM NaCl, 15 mM Na citrate, pH 7.0), eggs were bleached with 1–2% H2O2 (ThermoFisher Scientific) in 0.5X SSC containing 5% formamide (Sigma) for 2–3 h under light, then washed in PBT (137 mM NaCl, 2.7 mM KCl, 10 mM Na2HPO4, 0.1% Triton X-100 [Thermo Fisher Scientific]) and 2 mg/mL bovine serum albumin (BSA). Eggs were blocked in PBT supplemented with 10% goat serum (Gibco–Thermo Fisher Scientific) and 5% DMSO for 1–3 h and incubated overnight at 4°C in PBT supplemented with 10% goat serum and primary antibodies. The following antibodies were used to label tubulin and DNA, respectively: 1:500 mouse anti-beta tubulin (E7; Developmental Studies Hybridoma Bank), and 1:500 rabbit anti-histone H3 (ab1791; Abeam). Eggs were then washed 4×2 hours in PBT and incubated overnight in PBT supplemented with 1:500 goat anti-mouse or goat anti-rabbit secondary antibodies coupled either to Alexa Fluor 488 or 568 (Invitrogen – ThermoFisher Scientific). Eggs were then washed 4×2 hours in PBT and gradually dehydrated in methanol. Eggs were cleared in Murray's clearing medium (2 parts Benzyl Benzoate, 1 part Benzyl Alcohol; Sigma). Cleared eggs were then mounted on a microscope slide, squashed under a coverslip, and imaged by epifluorescence microscopy.

Xenopus egg extract preparation

Xenopus laevis and *Xenopus tropicalis* egg extracts were prepared as previously described [1,18]. Briefly, eggs in metaphase of meiosis II were collected, dejellied and fractionated by centrifugation. The cytoplasmic layer was isolated, supplemented with 10 mg/mL each of the protease inhibitors leupeptin, pepstatin and chymostatin (LPC), 20 mM cytochalasin D, and a creatine phosphate and ATP energy regeneration mix, and stored on ice (X. *laevis*) or at room temp (X. *tropicalis*) for up to 6 hours. Typical spindle reactions contained 25 μL CSF extract, *X. laevis* or *X. tropicalis* sperm at a final concentration of 500 nuclei per μl, and rhodamine-labeled porcine brain tubulin at a final concentration of 50 μg/ml.

H. boettgeri egg extract preparation

Methods for working with *H. boettgeri* were generally based on those described in [19,20]. 8–12 H. boettgeri females were injected in the dorsal lymph sac with 200 units HCG (Sigma, in a limited volume of 100 μL) 16 hours before egg collection. Frogs were housed overnight at room temperature in distilled deionized water (ddW). Eggs were dejellied using a solution of 2% cysteine and 0.1% bovine serum albumin (BSA) in ddW adjusted to pH 7.8.

Eggs were then washed extensively in CSF-XB buffer (5 mM EGTA, 100 mM KCl, 3 mM MgCl2, 0.1 mM CaCl2, 50 mM sucrose, and 10 mM HEPES pH 7.7) plus protease inhibitors (leupeptin, pepstatin, and chymostatin, 10 μg/ml each) and cytochalasin D (20 μg/ml), then packed by centrifugation in a 1.5 -ml microfuge tube at 1000×*g* for 1 min followed by 2000×*g* for 10 s. All buffer was removed, and eggs were crushed by centrifugation at 17,000×*g* for 15 min in a swinging bucket rotor (Sorvall HB-6, Thermo Fisher Scientific). Concentrated cytoplasm was removed from the tube and immediately placed at room temperature. Additional protease inhibitors, cytochlasin D, and energy mix were added as for *Xenopus* egg extracts. Typical spindle reactions contained 25 μL CSF extract, *H. boettgeri* sperm at a final concentration of 500 nuclei per μl, and rhodamine-labeled porcine brain tubulin at a final concentration of 50 μg/ml.

Immunofluorescence of spindles in egg extracts

Spindle reactions were processed as described in [18]. Briefly, 25 μl egg extract reactions were fixed by addition to 1 ml of dilution buffer (80 mM Pipes, 1 mM $MgCl_2$, 1 mM EGTA, 30% glycerol, 0.5% Triton X-100, and 2.5% formaldehyde). After incubating for 10 min at 23°C, samples were spun onto coverslips through a 5-ml cushion (BRB80 + 40% glycerol) at 10,200 rpm for 15 min using a swinging bucket rotor (Sorvall HB-6). Coverslips were postfixed for 5 min in 100% methanol, rinsed with PBS-0.1%NP40, blocked with PBS–1% BSA for 45 min, and incubated with primary antibody against TPX2 (diluted 1: 2500 in PBS–1% BSA) or kif2a (diluted 1: 5,000 in PBS–1% BSA) overnight in a humidified container at 4°C. Coverslips were rinsed 3x with PBS-0.1%NP40, then incubated for 45 min at room temp with secondary antibody (Invitrogen; Goat anti-rabbit or mouse anti-human IGG conjugated to Alexa Fluor 488, used at a 1:1000 dilution). Coverslips were then stained with 5 μg/ml Hoechst 33258 (Sigma), and mounted on microscope slides using Vectashield (Vector Laboratories).

Microscopy, image processing, and spindle measurement

Images were obtained on a fluorescence microscope (BX51; Olympus) with TRITC, DAPI, and FITC filters (Chroma Technology Corp.) and a 20 or 40x objective (0.75 NA; UPlanFl N; Olympus) controlled by μManager software (http://www.micromanaqer.org/) with an Orca-ER cooled charge-coupled device camera (Hamamatsu Photonics). Spindle length was measured using pole-to-pole distance with the line tool in Fiji [21]. Fluorescence intensity line scans were generated using an automated Java ImageJ plugin developed by X. Zhou (https://github.com/XiaoMutt/AiSpindle) [22].

Western blots

Egg extract protein concentrations were measured by Bradford assay (Biorad). Decreasing volumes of *X. laevis, X. tropicalis*, or *H. boettgeri* egg extracts (corresponding to 50, 25, and 12.5 μg total protein per lane) were separated by SDS-PAGE and wet transferred to nitrocellulose membrane (BioRad). Blots were blocked with PBS-0.1%Tween+ 5% milk for 45 min, probed with primary antibodies diluted in PBS-0.1%Tween+ 5% milk overnight at 4°C, rinsed 3x over a 10 minute period at room temp with PBS-0.1%Tween, then probed with secondary antibodies diluted in PBS-0.1%Tween (Rockland Immunochemicals ; goat anti–rabbit DyLight 800, goat anti-human DyLight 800, or donkey anti–mouse DyLight 680,

all used at a 1:10,000 dilution). Blots were scanned on an Odyssey Infrared Imaging System (LI-COR Biosciences). Band intensities were quantified using Fiji.

Antibody inhibition of Kif2a in *H. boettgeri* egg extracts

An antibody raised against an N-terminal sequence of human kif2a (Novus Biologicals) was added to *H. boettgeri* egg extracts at a final concentration of 0.7 mg/ml. Rabbit IGG was added to control reactions at a final concentration of 0.7 mg/ml. Egg extract reactions were then fixed and sedimented onto coverslips as described for immunofluorescence above.

RNA Isolation and Sequencing

To isolate RNA, *H. boettgeri* eggs and embryos at stage 14 were homogenized mechanically in TRIzol® (Thermo Fisher Scientific) using a 30-gauge needle and processed according to manufacturer instructions. After resuspension in nuclease-free H2O, RNAs were isolated using a RNeasy kit (Qiagen Inc.) according to manufacturer instructions. Libraries were prepared using the manufacturer's non-standard specific RNA-seq library protocol with poly-A capturing mRNA enrichment method (Illumina, CA, USA). The paired-end 2 × 100 bp reads were generated by the QB3 Functional Genomics Laboratory at the University of California, Berkeley using Illumina HiSeq 2000.

H. boettgeri transcriptome assembly

H. boettgeri RNAseq reads from each library were assembled using Trinity [23] with default parameters for a denovo assembly. The complete transcriptome was aligned to *X. tropicalis* v9 proteome via BLASTX [24]. For each *X. tropicalis* protein, the highest scoring (based on BLAST bit score), transcript that aligned across the full-length (90% of the CDS) was chosen as the representative homolog for *H. boettgeri*. The raw RNA-seq data and initial Trinity assemblies were deposited at NCBI under BioProject PRJNA306175 [4].

Vertebrate sequence alignments

Vertebrate sequences for katanin and kif2a were aligned using Dialign-TX [25]. *X. tropicalis* and *X. laevis* cDNA and peptide sequences were obtained from Xenbase (version 9 genomes). Human, chicken, and lizard peptides were obtained from Ensembl (version 96; [26]. *Nanorana parkeri* sequences were obtained from Sun et al [27]. *Rana pipiens* sequences were obtained from Christenson et al. [28]. *X. borealis* cDNA sequences were kindly provided by Austin Mudd (UC Berkeley).

Cloning of *X. laevis* and *H. boettgeri* kif2a

Recombinant full length wild type *X. laevis* kif2a in a pMal- c5x vector (from New England BioLabs, further described in [8]) was used in this study. This construct was also used as a template to generate *X. laevis* kif2a point mutants (Kif2a I252S, Kif2a I252E).

To generate the wild type H. boettgeri kif2a construct, total RNA was isolated from *H. boettgeri* eggs as described above in "RNA isolation and sequencing," and cDNA was synthesized from RNA using the Superscript III First Strand Synthesis system (Thermo Fisher Scientific) according to the manufacturer's instructions. The *H. boettgeri* kif2a sequence was then PCR-amplified from the cDNA. The amplified sequence was then

subcloned into a pMal-c5x vector (New England BioLabs) using In-Fusion cloning (Takara). The construct was then amplified using XL1-Blue competent *E. coli* (Agilent). All point mutants (Kif2a I252S, Kif2a S252I, Kif2a I252E) were generated using a QuikChange Site Directed Mutagenesis Kit (Agilent).

Expression and purification of recombinant kif2a

Recombinant N-terminally MBP-tagged full length *X. laevis* and *H. boettgeri* kif2a and point mutants (all in a pMal- c5x vector from New England BioLabs, *X. laevis* construct is further described in [8]) were expressed in One Shot BL21 Star E. coli (Thermo Fisher Scientific) overnight with shaking at 16°C in the presence of 1 mM IPTG. Purification of *X. laevis* kif2a was originally described in [8] and purification of *H. boettgeri* kif2a and point mutants proceeded similarly. Bacteria were pelleted and lysed in Kif2a Purification Buffer containing 20 mM Hepes, 250mM NaCl, 1 mM DTT, pH7.2. To reduce viscosity of lysate and to limit proteolysis, Lysonase Bioprocessing Reagent (EMD Millipore) and Complete EDTA-free Protease Inhibitor Tablets (Roche) were added to the lysis buffer according to the manufacturer's instructions. Bacteria were lysed using sonication, then the clarified lysate incubated with amylose resin (New England Biolabs) for 40 min with rotation at 4°C. The amylose resin was then thoroughly rinsed with Kif2a Purification Buffer and the recombinant kif2a eluted with Kif2a Purification Buffer + 10 mM maltose. The most concentrated fractions were pooled and then buffer-exchanged into Kif2a Purification Buffer using Amicon Ultra Centrifugal filters, 15 ml, 30K MWCO (EMD Millpore) according to the manufacturer's instructions.

Time lapse microtubule depolymerization assay in frog egg extracts

Microtubules were polymerized from unlabeled + Alexa488-labeled porcine brain tubulin at a ratio of 20:1 unlabeled:labeled tubulin using taxol (Paclitaxel, Sigma) as described [29]. Flow cells were constructed with an 18 × 18 glass coverslip and double-sided Scotch tape for a volume of ~10 μl. A mutant rigor kinesin [30] in KAB (20 mM HEPES pH 7.5, 25 mM K-glutamate, 2 mM $MgCl_2$, 1 mg/ml BSA, 10% glycerol, 0.02% Triton X-100) with 1 mM ATP [31] was incubated in the flow cell. The cell was washed with KAB, incubated with microtubuless in KAB with ATP, and washed with BRB80 (80 mM PIPES [pH 6.8], 1 mM $MgCl_2$, 1 mM EGTA). Finally, 18–20 μl of crude egg extract was flowed in and immediately imaged at 15 s intervals with a 60× oil objective. Percent microtubule intensity was quantified by measuring the total integrated fluorescence intensity of each image per unit time using Fiji software.

Microtubule sedimentation assay using recombinant kif2a

5 μM Taxol- stabilized microtubules were generated as described in [29]. Microtubules were then incubated at room temp for 20 min with 200–400 nM recombinant *X. laevis* or *H. boettgeri* kif2a + 1.5 mM MgATP, or 200–400 nM Kif2a Purification Buffer (control) containing 20 mM Hepes, 250mM NaCl, 1 mM DTT, pH7.2. Total reaction volume was 25 μl. Reactions were layered onto 200 μl of a 40% sucrose/1× BRB80 cushion and sedimented at 23°C at 40,000 rpm for 20 min in a TL-100 rotor. Samples were taken of the supernatant (30 μl), the supernatant aspirated, the interface between the supernatant and the cushion washed with 100 μl dH2O, the cushion aspirated and the pellet resuspended in 30 μl

Laemmli sample buffer. Samples were then run on a 4–20% SDS-PAGE gradient gel (Biorad) and stained with Coomassie Blue.

Antibodies

Anti-TPX2: A rabbit polyclonal antibody against a 242 amino acid sequence in the N-terminus of *X. laevis* TPX2 was raised by Covance and affinity purified from total serum on a HiTrap *N*-hydroxysuccinimide–activated HP column (GE Healthcare) coupled with recombinant full length *X. laevis* TPX2. Antibodies were eluted with Gentle Ag/Ab Elution Buffer (Thermo Fisher Scientific) and dialyzed into 50 mM Hepes. The 242 amino acid sequence is highly conserved between *X. laevis* and *X. tropicalis* (87% identical) and *X. laevis* and *H. boettgeri* (86% identical), and was used at a 1:5,000 dilution for Western blot, and a 1:5,000 dilution for immunofluorescence.

Anti-kif2a: A rabbit polyclonal antibody raised against an N-terminal sequence of human kif2a (Novus Biologicals; 91% identical to *X. laevis* and *H. boettgeri* kif2a, 93% identical *to X. tropicalis* kif2a). Used at a 1:10,000 dilution for Western blot, and a 1:5,000 dilution for immunofluorescence.

Anti-Ran: A mouse polyclonal antibody (BD Biosciences) raised against amino acids 7–171 of human Ran. Within this region the *X. laevis, X. tropicalis*, and *H. boettgeri* sequences are identical. Used at a 1:2,000 dilution for Western blot.

Anti-beta-tubulin: A mouse monoclonal antibody (E7; Developmental Studies Hybridoma Bank, Iowa City, IA) raised against full length chlamydomonas tubulin. Used at a 1:500 dilution for whole-mount immunofluorescence.

Anti-histone H3: A rabbit polyclonal antibody (ab1791; Abcam) raised against amino acids 100–136 of human histone H3. Used at a 1:500 dilution for whole-mount immunofluorescence.

Anti-katanin: A rabbit polyclonal antibody raised against full length p60 subunit of *X. tropicalis* katanin [32]. Used at a 1:1000 dilution for Western blot.

Quantification and statistical analysis

Quantification of spindle length: Individual spindle lengths are represented by box plots in figures. For all box plots, the thick line inside the box indicates the average length, and the upper and lower box boundaries indicate the standard deviation (std dev). For each figure, the minimum number of spindles measured (n) as well as the number of eggs or egg extracts used are listed in the figure legend. Statistical significance was determined by unpaired two sample t-test in Microsoft Excel, and p values are listed in the figure legend.

Quantification of fluorescence intensity line scans: Line scans quantify the average ratio of kif2a to tubulin fluorescence intensity across the spindle length in each species egg extract. The minimum number of spindles measured in each condition (n) as well as the number of egg extracts used are listed in the figure legend. Error bars indicate +/`standard deviation (std dev).

Data and code availability

Raw *H. boettgeri* RNA-seq data and initial Trinity assemblies used in this study are publicly available at NCBI under BioProject PRJNA306175 https://www.ncbi.nlm.nih.gov/bioproject/306175 [4].

Supplementary Material

Refer to Web version on PubMed Central for supplementary material.

Acknowledgements

We thank students Rebecca Lamothe, Mike Fitzsimmons, and Sophie Kawada for dedicated assistance to K.M. with experiments. We also thank Sofia Medina Ruiz for assistance with *H. boettgeri* transcriptome assembly, and Austin Mudd for kif2a and katanin sequences in *Xenopus borealis*. We thank Dan Rokhsar for advice and assistance throughout this project. We thank all Heald lab members, past and present, for valuable advice, feedback, and support throughout this project. K. M. was supported by an NSF GRFP fellowship. R.H. was supported by NIH MIRA grant R35 GM118183 and the Flora Lamson Hewlett Chair.

References

1. Brown KS, Blower MD, Maresca TJ, Grammer TC, Harland RM, and Heald R (2007). Xenopus tropicalis egg extracts provide insight into scaling of the mitotic spindle. J. Cell Biol 176, 765–770. [PubMed: 17339377]
2. Loughlin R, Wilbur JD, McNally FJ, Nedelec FJ, and Heald R (2011). Katanin contributes to interspecies spindle length scaling in xenopus. Cell 147, 1397–1407. [PubMed: 22153081]
3. Helmke KJ, and Heald R (2014). TPX2 levels modulate meiotic spindle size and architecture in Xenopus egg extracts. J. Cell Biol 206, 385–393. [PubMed: 25070954]
4. Session AM, Uno Y, Kwon T, Chapman JA, Toyoda A, Takahashi S, Fukui A, Hikosaka A, Suzuki A, Kondo M, et al. (2016). Genome evolution in the allotetraploid frog Xenopus laevis. Nature 538, 336–343. [PubMed: 27762356]
5. Feng Y-J, Blackburn DC, Liang D, Hillis DM, Wake DB, Cannatella DC, and Zhang P (2017). Phylogenomics reveals rapid, simultaneous diversification of three major clades of Gondwanan frogs at the Cretaceous–Paleogene boundary. Proc. Natl. Acad. Sci 114, E5864–E5870. [PubMed: 28673970]
6. Buster D, McNally K, and McNally FJ (2002). Katanin inhibition prevents the redistribution of gamma-tubulin at mitosis. J. Cell Sci 115, 1083–92. [PubMed: 11870226]
7. Zhang D, Grode KD, Stewman SF, Diaz-Valencia JD, Liebling E, Rath U, Riera T, Currie JD, Buster DW, Asenjo AB, et al. (2011). Drosophila katanin is a microtubule depolymerase that regulates cortical-microtubule plus-end interactions and cell migration. Nat. Cell Biol 13, 361–372. [PubMed: 21378981]
8. Wilbur JD, and Heald R (2013). Mitotic spindle scaling during Xenopus development by kif2a and importin α. Elife 2, e00290. [PubMed: 23425906]
9. Trofimova D, Paydar M, Zara A, Talje L, Kwok BH, and Allingham JS (2018). Ternary complex of Kif2A-bound tandem tubulin heterodimers represents a kinesin-13-mediated microtubule depolymerization reaction intermediate. Nat. Commun 9, 10.1038/s41467-018-05025-7.
10. Miyamoto T, Hosoba K, Ochiai H, Royba E, Izumi H, Sakuma T, Yamamoto T, Dynlacht BD, and Matsuura S (2015). The Microtubule-Depolymerizing activity of a mitotic kinesin protein KIF2A drives primary cilia disassembly coupled with cell proliferation. Cell Rep. 10, 664–673. [PubMed: 25660017]
11. Jang C-Y, Coppinger J. a, Seki A, Yates JR, and Fang G (2009). Plk1 and Aurora A regulate the depolymerase activity and the cellular localization of Kif2a. J.CellSci 122, 1334–1341.
12. Loughlin R, Heald R, and Nédélec F (2010). A computational model predicts Xenopus meiotic spindle organization. J. Cell Biol 191, 1239–1249. [PubMed: 21173114]

13. Kitaoka M, Heald R, and Gibeaux R (2018). Spindle assembly in egg extracts of the Marsabit clawed frog, Xenopus borealis. Cytoskeleton 75, 244–257. [PubMed: 29573195]
14. Reber SB, Baumgart J, Widlund PO, Pozniakovsky A, Howard J, Hyman AA, and Jülicher F (2013). XMAP215 activity sets spindle length by controlling the total mass of spindle microtubules. Nat. Cell Biol 15, 1116–1122. [PubMed: 23974040]
15. Goshima G, and Scholey JM (2010). Control of Mitotic Spindle Length. Annu. Rev. Cell Dev. Biol 26, 21–57. [PubMed: 20604709]
16. Crowder ME, Strzelecka M, Wilbur JD, Good MC, vonDassow G, and Heald R (2015). A Comparative Analysis of Spindle Morphometrics across Metazoans. Curr. Biol 25, 1542–1550. Available at: http://dx.doi.Org/10.1016/j.cub.2015.04.036. [PubMed: 26004761]
17. Lee C, Kieserman E, Gray RS, Park TJ, and Wallingford J (2008). Whole-mount fluorescence immunocytochemistry on Xenopus embryos. CSH Protoc. 2008, pdb.prot4957.
18. Hannak E, and Heald R (2006). Investigating mitotic spindle assembly and function in vitro using Xenopus laevis egg extracts. Nat. Protoc 1, 2305–14. Available at: http://www.ncbi.nlm.nih.gov/pubmed/17406472. [PubMed: 17406472]
19. Minsuk SB, and Keller RE (1996). Dorsal mesoderm has a dual origin and forms by a novel mechanism in Hymenochirus, a relative of Xenopus. Dev. Biol 174, 92–103. Available at: http://www.ncbi.nlm.nih.gov/pubmed/8626024. [PubMed: 8626024]
20. Minsuk SB, and Keller RE (1997). Surface mesoderm in Xenopus: A revision of the stage 10 fate map. Dev. Genes Evol 207, 389–401. [PubMed: 27747438]
21. Schindelin J, Arganda-Carreras I, Frise E, Kaynig V, Longair M, Pietzsch T, Preibisch S, Rueden C, Saalfeld S, Schmid B, et al. (2012). Fiji: An open-source platform for biological-image analysis. Nat. Methods 9, 676–682. [PubMed: 22743772]
22. Gibeaux R, Acker R, Kitaoka M, Georgiou G, Van Kruijsbergen I, Ford B, Marcotte EM, Nomura DK, Kwon T, Veenstra GJC, et al. (2018). Paternal chromosome loss and metabolic crisis contribute to hybrid inviability in Xenopus. Nature 553, 337–341. [PubMed: 29320479]
23. Grabherr MG, Haas BJ, Yassour M, Levin JZ, Thompson DA, Amit I, Adiconis X, Fan L, Raychowdhury R, Zeng Q, et al. (2011). Full-length transcriptome assembly from RNA-Seq data without a reference genome. Nat. Biotechnol 29, 644–652. [PubMed: 21572440]
24. Camacho C, Coulouris G, Avagyan V, Ma N, Papadopoulos J, Bealer K, and Madden TL (2009). BLAST+: Architecture and applications. BMC Bioinformatics 10.
25. Subramanian AR, Kaufmann M, and Morgenstern B (2008). DIALIGN-TX: Greedy and progressive approaches for segment-based multiple sequence alignment. Algorithms Mol. Biol 3, doi:10.1186/1748-7188-3-6.
26. Zerbino DR, Achuthan P, Akanni W, Amode MR, Barrell D, Bhai J, Billis K, Cummins C, Gall A, Girón CG, et al. (2018). Ensembl 2018. Nucleic Acids Res. 46, D754–D761. [PubMed: 29155950]
27. Sun Y-B, Xiong Z-J, Xiang X-Y, Liu S-P, Zhou W-W, Tu X-L, Zhong L, Wang L, Wu D-D, Zhang B-L, et al. (2015). Whole-genome sequence of the Tibetan frog Nanorana parkeri and the comparative evolution of tetrapod genomes. Proc. Natl. Acad. Sci 112, E1257–E1262. [PubMed: 25733869]
28. Christenson MK, Trease AJ, Potluri L-P, Jezewski AJ, Davis VM, Knight LA, Kolok AS, and Davis PH (2014). De novo Assembly and Analysis of the Northern Leopard Frog Rana pipiens Transcriptome. J. Genomics 2, 141–149. [PubMed: 25371763]
29. Hyman A, Drechsel D, Kellogg D, Salser S, Sawin K, Steffen P, Wordeman L, and Mitchison T (1991). Preparation of modified tubulins. Methods Enzymol. 196, 478–485. [PubMed: 2034137]
30. McNally FJ, and Thomas S (1998). Katanin is responsible for the M-phase microtubule-severing activity in Xenopus eggs. Mol. Biol. Cell 9, 1847–61. [PubMed: 9658175]
31. Hartman JJ, Mahr J, McNally K, Okawa K, Iwamatsu A, Thomas S, Cheesman S, Heuser J, Vale RD, and McNally FJ (1998). Katanin, a microtubule-severing protein, is a novel AAA ATPase that targets to the centrosome using a WD40-containing subunit. Cell 93, 277–287. [PubMed: 9568719]
32. Loughlin R, Wilbur JD, McNally FJ, Nédélec FJ, and Heald R (2011). Katanin contributes to interspecies spindle length scaling in xenopus. Cell 147, 1397–1407. [PubMed: 22153081]

Highlights

- Egg extracts from the tiny frog *H. boettgeri* reconstitute spindle assembly in vitro
- Spindle size scaling mechanisms differ from those of *X. laevis* and *X. tropicalis*
- The microtubule depolymerizing motor kif2a regulates spindle length in *H. boettgeri*
- Interspecies variation in phosphorylation sites contributes to scaling mechanisms

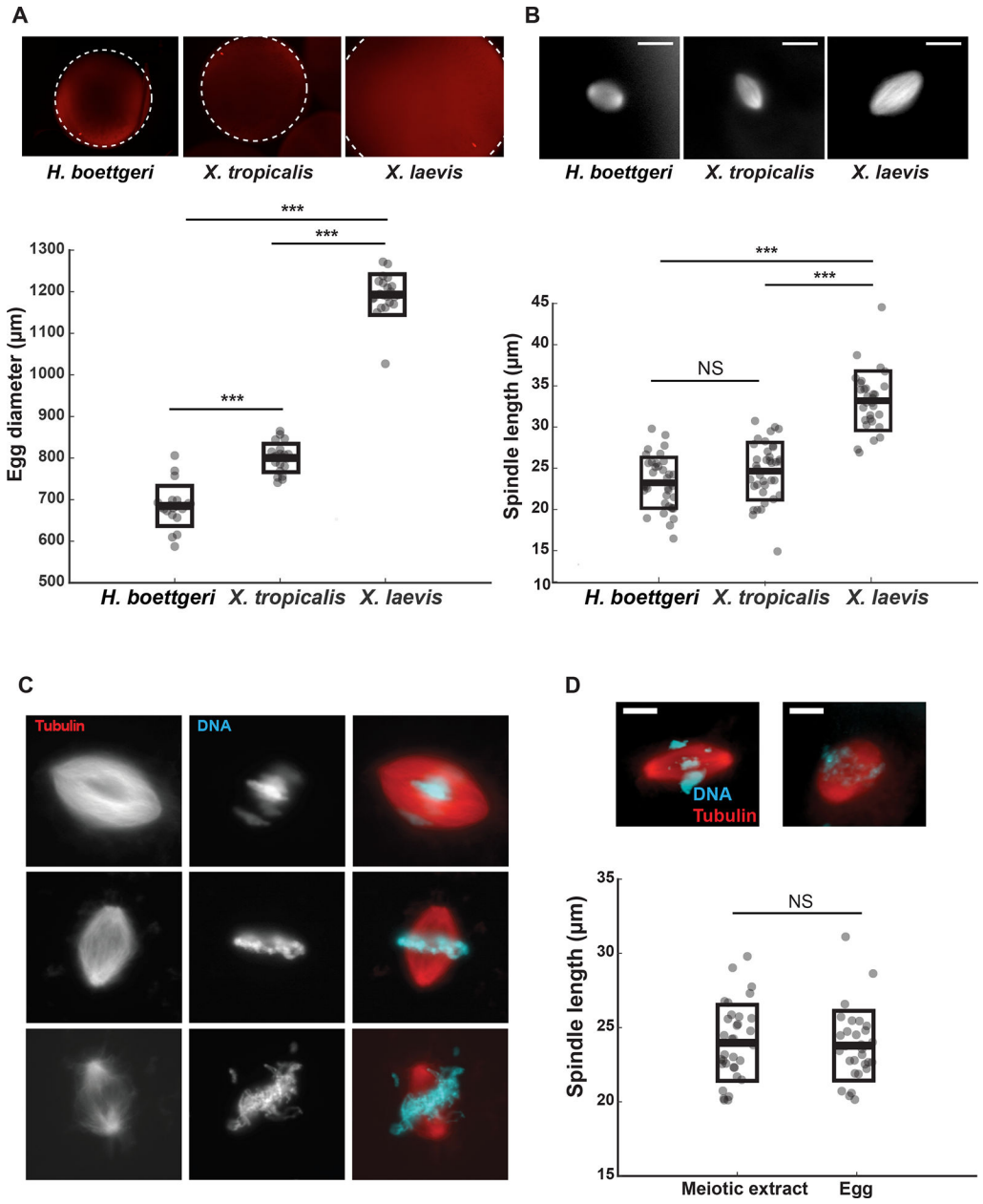

Figure 1: Comparison of meiotic spindle length in Pipid frog species

A. Immunofluorescence images and egg diameter quantification of fixed eggs of each frog species. Box plot shows all individual egg diameters. n≥20 egg diameters measured for each species. B. Comparison of meiotic spindle length of *X. laevis, X. tropicalis*, and *H. boettgeri*, measured by immunofluorescence in fixed eggs. n>30 spindles for each species. Box plot shows all individual spindle lengths. C. Representative images of spindles assembled in *X. laevis, X. tropicalis*, and *H. boettgeri* egg extracts. D. Spindle length measured in either fixed *H. boettgeri* eggs in vivo or *H. boettgeri* egg extracts in vitro. n=30 egg spindles, n=38 extract spindles from 3 separate *H. boettgeri* extracts. Box plot shows all individual spindle lengths. p= 0.426. For all box plots, thick line inside box= average length, upper and lower

box boundaries= +/− std dev. ***p<0.0001, NS= not significant. All scale bars = 10 μm. See also Figure S1A.

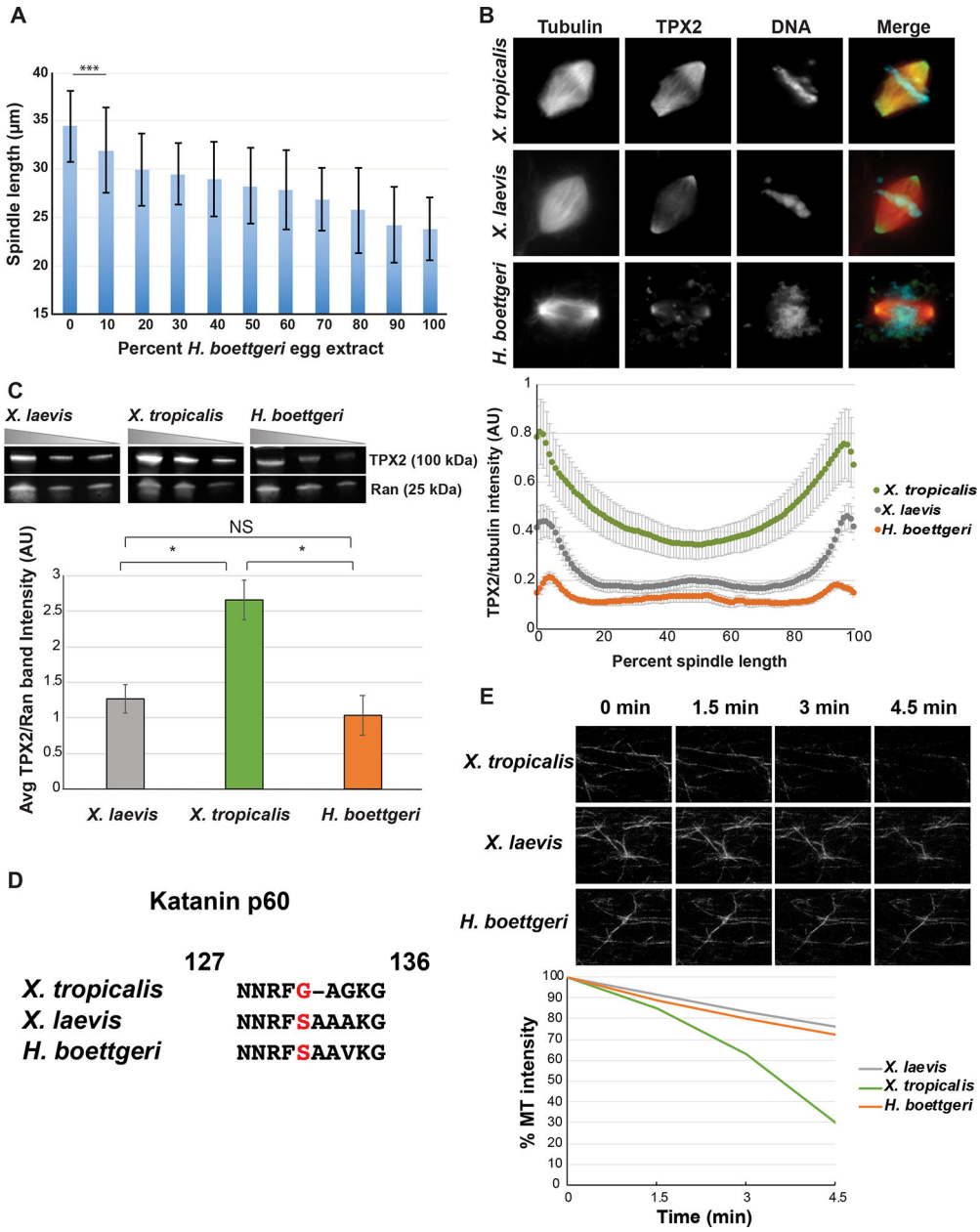

Figure 2: Cytoplasmic factors scale spindle length in *H. boettgeri* egg extracts through a mechanism distinct from that of *Xenopus* species

A. Quantification of spindle length in *X. laevis* extract mixed with increasing amounts of *H. boettgeri* extract. n>25 spindles each condition from 3 separate mixing experiments using 3 separate *X. laevis* egg extracts and 3 separate *H. boettgeri* extracts. Error bars= +/− std dev. There was a significant decrease in spindle length at 10% *H. boettgeri* egg extract added, ***p=0.0059. B. Top Panel: Representative immunofluorescence images of TPX2-stained spindles in *X. laevis, X. tropicalis*, and *H. boettgeri* egg extracts. Bottom Panel: Line scan quantification of the average ratio of TPX2 to tubulin fluorescence intensity across the spindle length in each species egg extract. n>50 spindles each extract from at least 3 extracts per species. Error bars= +/− std dev. AU=arbitrary units. C. Top Panel: Western blot of *X.*

laevis, X. tropicalis, and *H. boettgeri* extracts, probed for TPX2. Bottom Panel: Quantification of 3 separate blots for each species. Band intensities were normalized to the integrated density of the corresponding Ran loading control. AU=arbitrary units. D. Alignment of sequences around serine 131 in *X. laevis, X. tropicalis*, and *H. boettgeri* katanin p60. E. Top Panel: Representative images of fluorescently-labeled microtubule severing over time in each species egg extract. Bottom Panel: Quantification of integrated fluorescence intensity of representative images shown over time in each species egg extract. Similar effects were observed in n≥3 egg extracts per species; one representative assay is quantified here. All scale bars= 10 μm. See also Figure S1B and Figure S4B.

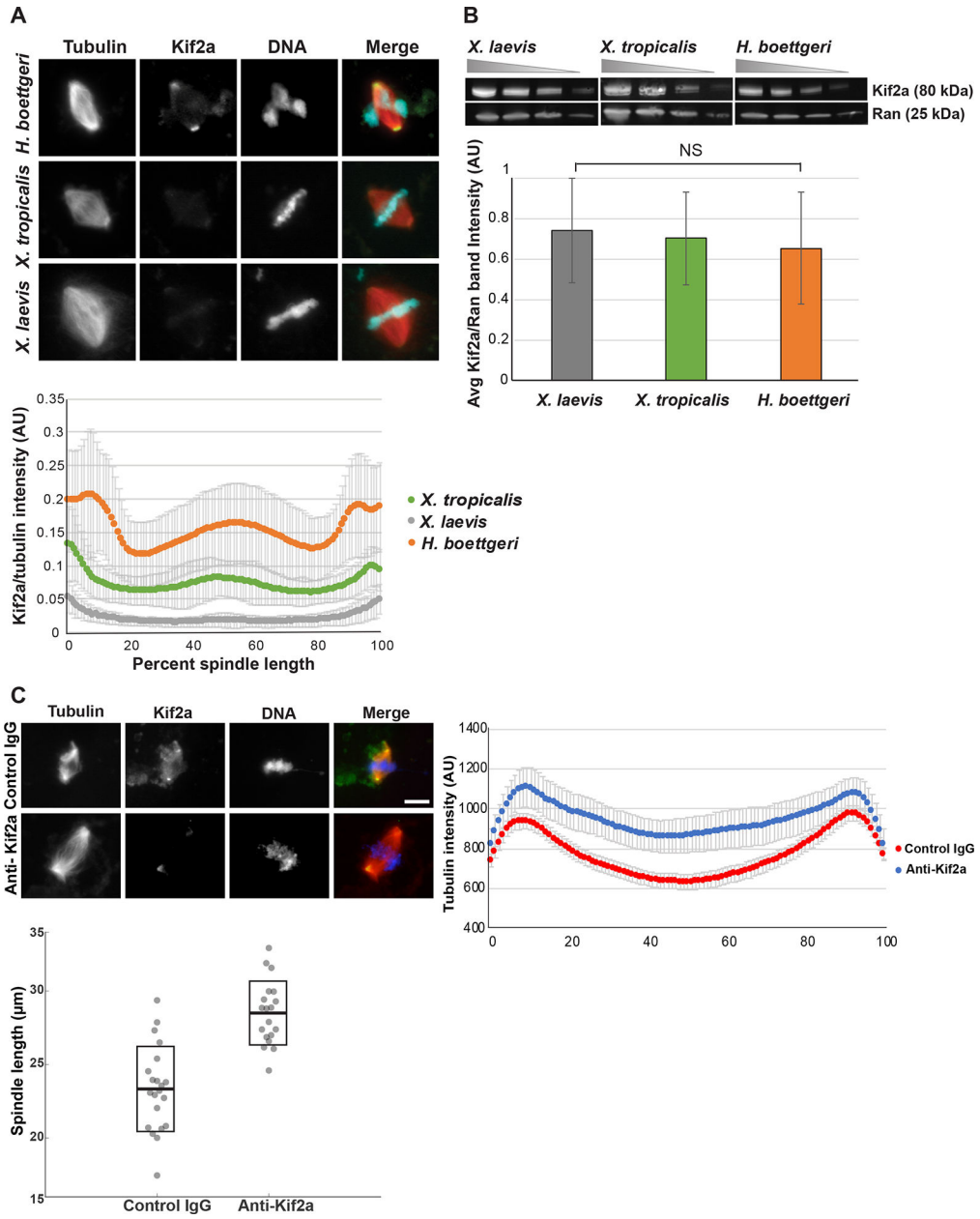

Figure 3: Kif2a is enriched on spindles in *H. boettgeri* egg extracts, and inhibition of kif2a increases spindle length.

Top Panel: Representative immunofluorescence images of kif2a-stained spindles in *X. laevis, X. tropicalis*, and *H. boettgeri* egg extracts. Bottom Panel: Line scan quantification of the average ratio of kif2a to tubulin fluorescence intensity across the spindle length in each species egg extract. n>50 spindles each extract from at least 3 extracts per species. Error bars= +/− std dev. B. Top Right Panel: Western blot of *X. laevis, X. tropicalis*, and *H. boettgeri* extracts, probed for kif2a. Bottom Panel: Quantification of 3 separate blots for each species. Band intensities were normalized to the integrated density of the corresponding Ran loading control. AU=arbitrary units. C. Top Left Panel: Representative spindle images in *H. boettgeri* egg extracts upon addition of a kif2a antibody or control IgG. Top Right Panel:

Line scan quantification of the average tubulin fluorescence intensity along the long axis of spindles in control- and kif2a-inhibited *H. boettgeri* egg extracts. AU=arbitrary units. Error bars= +/− std dev. Bottom Left Panel: Quantification of spindle length in kif2a inhibited *H. boettgeri* egg extracts. n≥19 spindles each from 2 extracts. Thick line inside box= average length, upper and lower box boundaries= +/− std dev. Kif2a antibody or control IgG were added to a final concentration of 0.7 mg/ml. Scale bars= 10 μm.

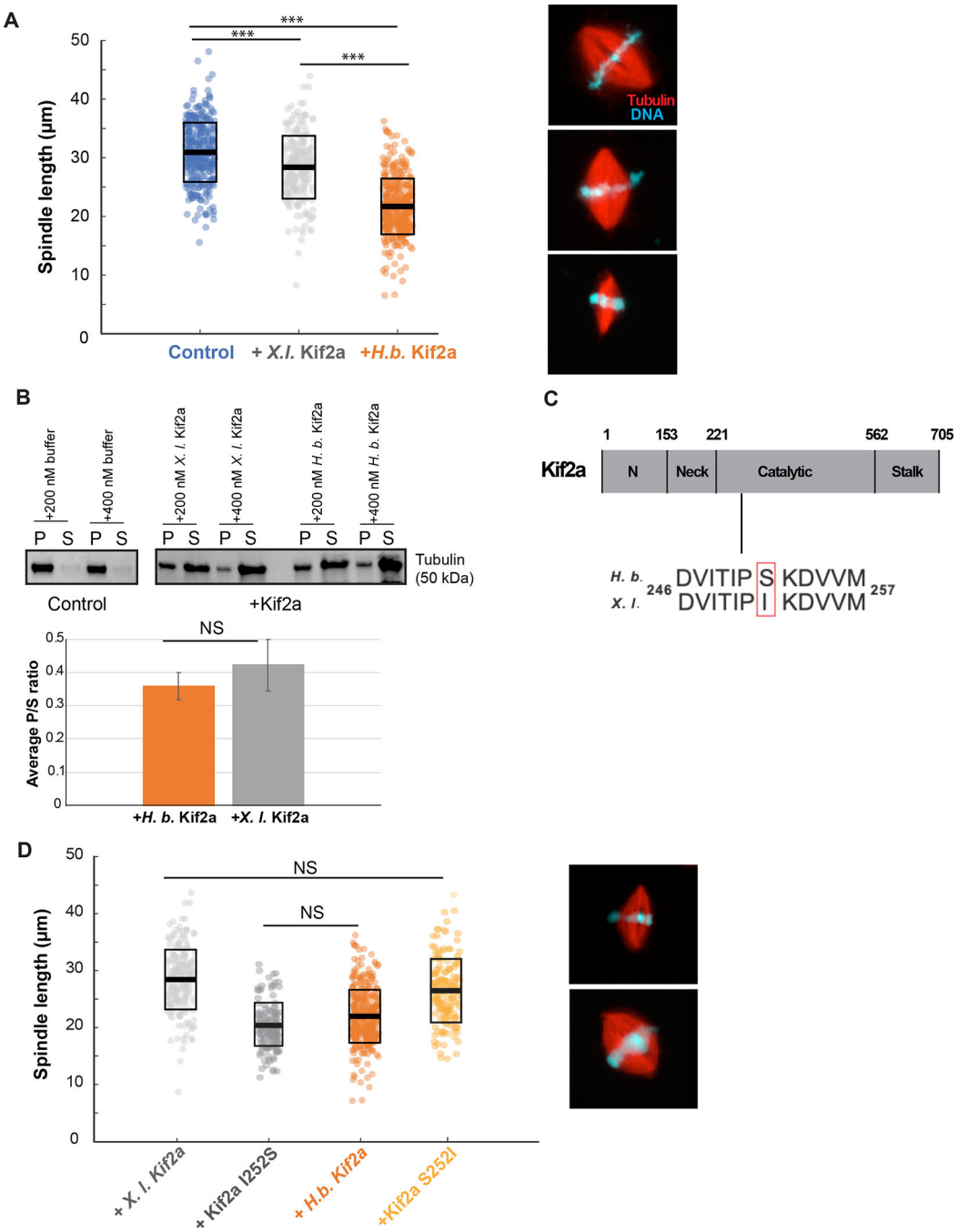

Figure 4: Serine 252 of kif2a regulates its activity

A. Left Panel: Spindle length in *X. laevis* egg extracts with 0.5 µM exogenous recombinant *X. laevis* or *H. boettgeri* proteins added. Right Panel: Representative images of spindles in (A). n≥137 spindles from 3 separate extracts. B. Top Panel: Increasing amounts of recombinant *X. laevis* or *H. boettgeri* kif2a proteins were added to taxol-stabilized microtubules and microtubules sedimented through a sucrose cushion. Amounts of soluble tubulin in the supernatant (S) and pellet (P) were quantified by SDS-PAGE and Coomassie staining. Bottom Panel: Ratio of pellet to supernatant gel band intensities in the microtubule

sedimentation assay with 200 nM *H. boettgeri* or *X. laevis* kif2a added. Bands from 3 separate gels quantified, p=0.2768. NS= Not Significant. Error bars= +/− std dev. C. Schematic of kif2a domain organization and sequence alignment of the area around amino acid 252 in *H. boettgeri* (*H.b.*), and *X. laevis* (*X.I.*). D. Left Panel: Spindle length in *X. laevis* egg extracts with 0.5 μM exogenous recombinant wildtype *X. laevis, H. boettgeri*, and mutant Kif2a I252S or Kif2a S252I proteins added. Right Panel: Representative images of spindles in (D). n≥138 spindles from 3 separate extracts. All box plots show all individual spindle lengths. Thick line inside box= average length, upper and lower box boundaries= +/− std dev. ***p<0.0001, NS=Not Significant. All scale bars=10 μm. See also Figure S2A, Figure S2B, Figure S3, and Figure S4A.